Kinematics of the Mw = 7.2, 12 November 1999, Düzce, Turkey Earthquake

M. E. Ayhan,[1] R. Bürgmann,[2] S. McClusky,[3] O. Lenk,[1] B. Aktug,[1] E. Herece,[4] and R. E. Reilinger[3]

Abstract. The November 12, 1999 Düzce earthquake ruptured a ∼40-km-long fault segment of the North Anatolian fault system immediately to the east of the August 17, 1999 Izmit rupture. We use displacements of 32 sites derived from GPS measurements immediately before and after the Düzce earthquake to estimate the geometry and slip distribution of the coseismic rupture. The ∼ 51° northward dipping rupture plane, the rake of the slip vector (average 3.76 ± 0.04 m right-lateral, 0.76 ± 0.04 m normal slip), and the slip distribution inferred from the GPS data are consistent with seismic observations and the distribution of surface offsets measured in the field. The geodetically determined moment magnitude is M_w = 7.2. The Düzce earthquake had the highest slip-to-rupture-length ratio of any historic earthquake along the North Anatolian fault. This is consistent with the Düzce earthquake being a part of a composite rupture with the preceding Izmit event.

Introduction

The November 12, M_w = 7.2 Düzce earthquake struck northwestern Turkey (Fig. 1) only 87 days after the August 17, 1999 Izmit earthquake (M_w = 7.5, [*Reilinger et al.*, 2000]), which was the largest and most destructive earthquake to occur along the North Anatolian fault (NAF) since 1939. The Düzce earthquake is the latest in a classic sequence of M ≥ 6.7 earthquakes that have propagated ∼1000 km along the NAF since the 1939 Erzincan earthquake [*Toksöz et al.*, 1979; *Barka*, 1996; *Stein et al.*, 1997].

The western NAF accommodates ∼25 mm/yr of right-lateral motion between Anatolia and Eurasia [*McClusky et al.*, 2000]. Near Bolu the NAF branches into a southern fault strand, which ruptured in M ≃ 7 earthquakes in 1957 and 1967 and the Düzce and Karadere fault segments to the north, bounding the uplifted Almacık block in between [*Sengör et al.*, 1985]. The northern strand has not ruptured in the 20th century [*Barka*, 1996]. Analysis of GPS data suggest that up to 10 mm/yr are accommodated on the Düzce-Karadere strand of the NAF [*Ayhan et al.*, 1999]. The Izmit earthquake ruptured the Karadere and westernmost Düzce segments (Fig. 1) and the Düzce earthquake ruptured most of the Düzce fault.

Focal mechanism determinations for the Düzce earthquake reveal a steeply N-dipping (55°-66°) nodal plane with a small component of normal slip, in addition to a dominant right-lateral component (Table 1, Fig. 1). Available hypocentral depth estimates range from 10 to 18 km (Table 1). Geologic investigations of the ∼40-km-long surface rupture reveal right-lateral offsets of up to 4.9 m, with subsidiary N-side-down vertical offsets along the western ∼15 km of the rupture. The western-most Düzce fault rupture also broke with minor (≤ 20 cm) right-lateral offsets in the preceding Izmit event.

Here, we use Global Positioning System (GPS) measurements of surface displacements during the Düzce earthquake to constrain the geometry and slip distribution of the rupture. Knowledge of the location and geometry of the rupture and of the distribution of coseismic fault slip provides basic information about the mechanics of the earthquake process and is important for better understanding of the role of the preceding Izmit earthquake in the timing and kinematics of the Düzce earthquake.

Coseismic surface displacements

A substantial GPS monitoring effort was underway prior to the Izmit-Düzce earthquake sequence to measure the strain accumulation along the NAF [*Straub et al.*, 1997; *McClusky et al.*, 2000]. Immediately following the August 17 Izmit earthquake, an effort was begun to re-measure the positions of many of the stations displaced by the earthquake and to monitor the post-earthquake deformation [*Reilinger et al.*, 2000]. On November 6, 1999, the General Command of Mapping commenced a survey of GPS stations around the Izmit rupture. The Düzce earthquake occurred on November 12, 1999, and the campaign was extended through November 19 to cover new stations around the Düzce rupture. Thus, most sites in the epicentral region had been surveyed within a week prior to the Düzce earthquake, and all were remeasured within a week following the event.

We processed the pre- and post-earthquake GPS data following procedures described by *McClusky et al.* [2000]. The pre-earthquake coordinates were corrected for post-Izmit earthquake transient deformation using their well-established time series or a detailed afterslip model [*Reilinger et al.*, 2000]. The largest correction for such preseismic deformation amounted to 11 mm over a 21-day time period. For continuously operating stations we difference coordinates from 2 days immediately before and 2 days after the event. Fig. 1 shows the estimated coseismic offsets and their 95% confidence ellipses.

[1]Department of Geodesy, General Command of Mapping, Ankara, Turkey
[2]Department of Earth and Planetary Science, University of California, Berkeley, California
[3]Department of Earth, Atmospheric, and Planetary Sciences, Massachusetts Institute of Technology, Cambridge, Massachusetts
[4]Department of Geology, General Directorate of Mineral Research and Exploration, Ankara, Turkey

Paper number 1999GL000000.
0094-8276/00/1999GL000000$05.00

Table 1. Fault Parameters for Geodetically Determined Models From Inversion of GPS Data

Model	Length (km)	Width (km)	Dip (°N)	Strike (°)	Lat. (°)	Lon. (°)	Dip slip (m ± 1 σ)	Strike slip (m ± 1 σ)	WRSS	Misfit	Mo (Nm)	Mw
1 fault	28.4	17.2	51	88	40.76	31.25	0.76 ± 0.04	3.76 ± 0.04	87	0.96	5.62E+19	7.17
Strike slip only	29.3	15.5	64	85	40.78	31.27		3.77 ± 0.04	242	1.62	5.15E+19	7.14
2 faults	15.6	19.5	64	82	40.76	31.12	0.42 ± 0.09	2.19 ± 0.07	56	0.63	5.27E+19	7.15
	10.1	16.2	45	95	40.76	31.32	2.08 ± 0.14	6.27 ± 0.12				
Distributed slip	50	21.8	51	88	40.76	31.21			73		5.86E+19	7.18
Seismic studies	Depth											
USGS NEIC	14		59	96	40.77	31.15					4.5E+19	7.1
Harvard CMT	18		54	88	40.93	31.25					6.7E+19	7.2
Yagi & Yiguchi	10		65	85	40.80	31.20					5.6E+19	7.1

Latitude and longitude refer to the center of surface fault trace or the moment tensor centroid.

Rupture geometry and slip distribution

The displacements of points at the Earth's surface caused by the Düzce earthquake reveal information about the rupture geometry and the distribution of fault slip. We model the observed coseismic displacements using rectangular dislocations in an elastic, homogeneous and isotropic half-space [Okada, 1985]. We use a constrained, nonlinear optimization algorithm [*Bürgmann et al.*, 1997], which allows us to estimate the geometry (parameterized by length, depth, width, dip, strike, and location) and the strike-slip and dip-slip offsets of one or more faults that best fit the GPS data. Our inversions attempt to minimize the weighted residual sum of squares $WRSS = (d_{obs} - d_{mod})^{\mathrm{T}} \times cov^{-1} \times (d_{obs} - d_{mod})$, where $(d_{obs} - d_{mod})$ are the differences of the observed and modeled displacement components or residuals and cov^{-1} is the inverse of the diagonal data covariance matrix, which determines the weighting of the residuals.

We find that the optimal uniform-slip dislocation closely follows the surface rupture mapped in the field and is consistent with seismologic evidence. The optimal model fault dips 51° to the north and slipped 3.76 m right-lateral and 0.76 m, N-side down (Table 1). Fig. 1 shows a comparison of observed and modeled station displacements for this 1-fault model. The geodetic moment magnitude of the Düzce earthquake is $M_w = 7.2$. Our measure of misfit, which accounts for the number of model parameters P and number of data N, $\sqrt{WRSS/(N-P)}$, also referred to as the reduced χ^2 value, for this model is 0.96 (Table 1). A misfit of 1 would indicate that the residuals are statistically consistent with the data errors. If we force the rupture to have strike slip only, the misfit substantially increases to 1.62 (Table 1). The Düzce earthquake had a significant normal faulting component in addition to the dominant strike slip, and occurred

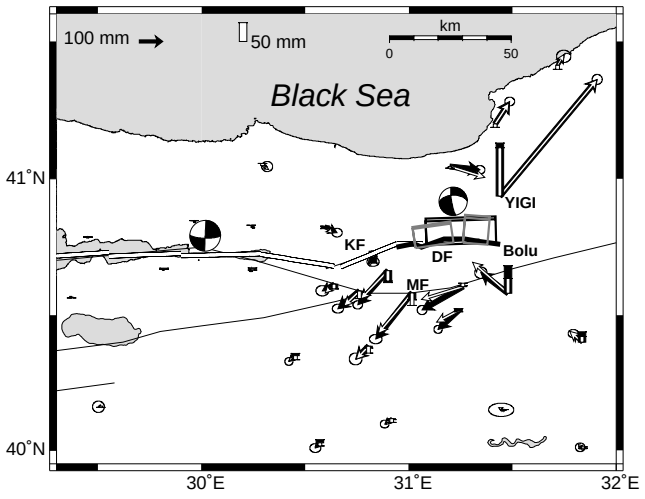

Figure 1. Map of Düzce region with observed coseismic displacements (filled arrows with 95% confidence ellipses) relative to a site in Ankara located at 39.89°N, 32.76°E. Open arrows are predicted displacements from single-dislocation model. Flat-tipped bars are vertical displacements (filled, observed; open, modeled). Double lines are segments of the Izmit earthquake rupture, the bold black line follows the Düzce surface rupture. KF, Karadere fault; MF, Mudurnu Valley fault segment; DF, Düzce fault. The black rectangle indicates the surface projection of the N-dipping dislocation, two gray rectangles show the best-fitting 2-fault model. Also shown are the focal mechanisms (Harvard moment tensor) of the Izmit and Düzce earthquakes.

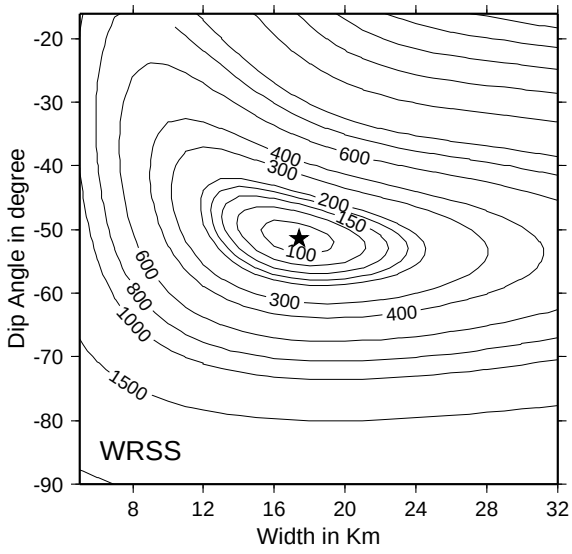

Figure 2. Contour plot of model misfit ($WRSS$) in dislocation dip - dislocation width parameter space. A northward dip of 48-53° and width of 16-20 km are favored.

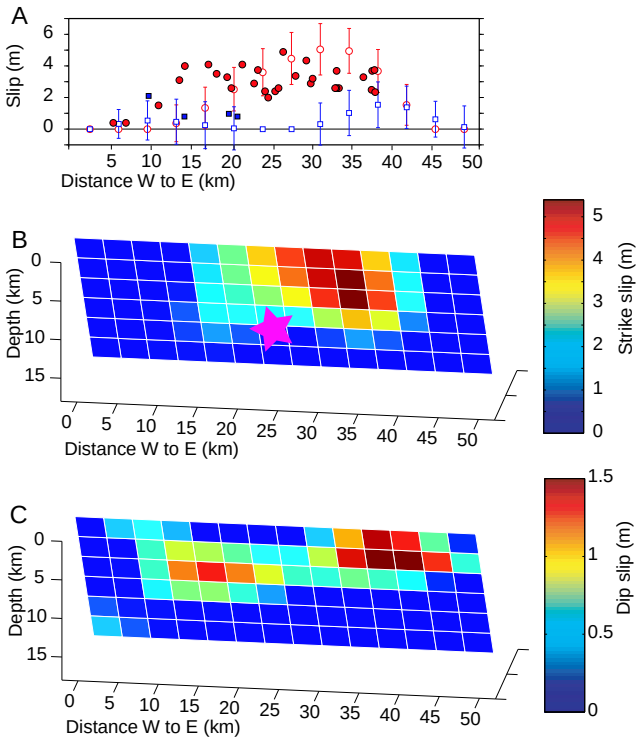

Figure 3. (A) Surface offsets from field measurements and model offsets on top row of slip patches. Solid red circles and blue squares are observed strike-slip and dip-slip offsets, respectively, open red circles and blue squares are modeled near-surface offsets. (B) Cross-section, perspective view from S of Düzce rupture strike-slip distribution. Pink star indicates Düzce earthquake hypocenter. (C) Normal-slip distribution.

on a north-dipping fault plane. To better understand how well we can constrain the steeply north-dipping rupture geometry, we evaluate the effects of rupture dip and width on the model misfit. Fig. 2 shows the contoured $WRSS$ as a function of width and dip of the uniform slip model fault. Fault dips from 48°-53° and widths from 16-20 km provide good fits to the geodetic data.

If we allow for a second dislocation in the geometry inversion, the rupture is separated into two adjoining segments where the eastern, smaller segment is favored to have significantly higher strike slip and dip slip (Table 1). The surface projections of the two dislocations are shown in Fig. 1 as blue rectangles. They closely follow the slight curvature of the surface rupture. Unless our estimates of the GPS displacement uncertainties are overly conservative, this model, and the distributed-slip model discussed below match the data better than required for an adequate fit (i.e., $\sqrt{WRSS/(N-P)} < 1$).

We evaluate a more detailed rupture model to determine if additional information about the coseismic slip distribution can be resolved with the GPS data. The mapped coseismic surface rupture and best-fit single-fault model determine the location and dip of the model fault. Our best-fitting single-fault model is enlarged at the down-dip and lateral edges and discretized into 3.6-km-long, 4.3-km-wide patches (14 by 6 elements) for the distributed slip inversions (Fig. 3). We invert for the optimal slip distribution and seek models that minimize the misfit, while preserving smoothness of the model slip distribution. We apply smoothing and non-negativity (right-lateral and normal slip only) constraints to avoid models with unreasonable (oscillating) slip patterns that are favored by a free inversion without such additional constraints [*Harris and Segall*, 1987].

Figs. 3 B and C show the strike-slip and dip-slip distribution most compatible, in a least squares sense, with the observed displacements. The distributed-slip model inversions resolve little additional detail and favor a simple slip model in which maximum strike slip occurs near the center and on the upper 15 km of the rupture and slip decays smoothly to the west and east. The slip distribution is somewhat skewed towards the east. Dip slip appears to be distributed on two regions and does not correlate well with the strike-slip distribution. As this model provides only a slightly better fit to the data than the uniform-slip model (Table 1), we believe that the Düzce earthquake was in fact a rather simple rupture, which is also indicated by teleseismic slip inversions [*Yagi and Kikuchi*, 1999]. Our maximum slip region is located just E of the hypocenter, whereas the seismic inversion shows the hypocenter to coincide with the high slip region. The distributed-slip model accounts for the large majority of the estimated site offsets (Fig. 4). The residuals of four sites along the easternmost Karadere segment of the August 17 Izmit earthquake rupture suggest that a small amount of strike slip could have been triggered by the Düzce event on that portion of the previous rupture.

Discussion and Conclusions

Our findings based on geodetic data are consistent with seismologic measurements. Inversions of teleseismic data for focal mechanisms suggest a 54-65° north-dipping nodal plane, somewhat steeper than our result (Table 1). A comparison of the distribution of coseismic slip with the

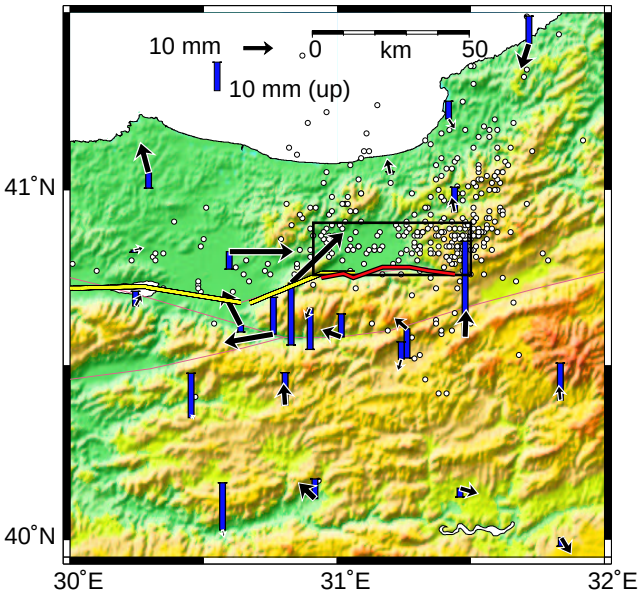

Figure 4. Residual (observed minus predicted) horizontal (black arrows) and vertical (blue, flat-tipped bars) station displacements from distributed-slip model shown in Fig. 3. The Düzce rupture follows the northern edge of an uplifted block between two strands of the NAF and a young basin to the north, as indicated by the shaded relief map of topography. Open circles are aftershock locations during first month following the event (from http://www.deprem.gov.tr).

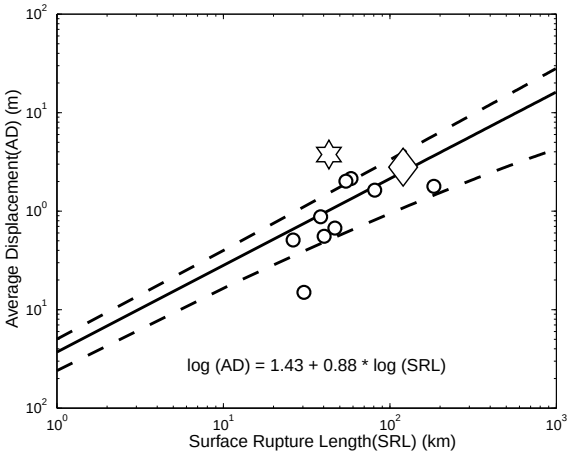

Figure 5. Rupture length vs. average fault slip for historic earthquakes along the NAF. Open circles are historic earthquakes since 1939 (from *Wells and Coppersmith* [1994]). The solid and dashed lines are the regression of rupture length on average slip established from a world-wide earthquake catalog and the 95% confidence bounds, respectively [*Wells and Coppersmith*, 1994]. The diamond indicates the Izmit rupture, the star the Düzce event. The Düzce earthquake has the highest slip-to-rupture-length ratio of any historic earthquake along the NAF.

hypocenter location indicates that the Düzce earthquake nucleated near the bottom center of the northward dipping rupture and propagated bilaterally east and west producing a relatively simple slip distribution (Fig. 3B). This result is consistent with teleseismic waveform inversions by *Yagi and Kikuchi* [1999]. The geodetic coseismic moment estimates of $M_o = 5.15 - 5.86 \times 10^{19}$ Nm ($M_w = 7.2$) lie within the range of seismic moments reported for the main shock ($M_o = 4.5 - 6.6 \times 10^{19}$ Nm). Slight differences in moment estimates might be caused by postseismic afterslip immediately following the earthquake, or could be due to other assumptions about the rheology of the crust and fault zone properties that go into the geodetic and seismic inversions.

The near-surface offsets of the distributed slip model can be compared to those observed by field measurements (Fig. 3A). We find a general confirmation of a relatively simple distribution with maximum slip of ∼5 m at ∼31.2° longitude. Whereas dip-slip offsets mapped in the field were restricted to the western half of the rupture, the geodetic inversion finds some dip slip further east. These discrepancies are likely due to the lack of GPS sites very close to the rupture, which limits our resolution of near-surface slip.

We find that the ratio of average (Fig. 5) and maximum slip to surface rupture length along the Düzce fault was higher than in any previous historic earthquake along the NAF [*Wells and Coppersmith*, 1994]. Our distributed-slip inversions and the distribution of aftershocks suggest that some subsurface slip might extend eastward past the ruptured surface trace (Fig. 3B and 4), but this alone can not explain the high slip-to-rupture-length ratio. The N-dipping fault geometry might further enhance the slip-to-rupture-length ratio, as it allows for a ∼15% larger rupture area for a given rupture length. However, this high ratio suggests to us that the Düzce earthquake was effectively part of a composite rupture with the preceding Izmit event and has a slip magnitude more consistent with the combined rupture length of ∼160 km.

Acknowledgments. This research was supported in part by MIT grants NSF INT-9724114 and NSF EAR-9909730. We thank TUBITAK MRC for providing GPS data from continuous stations of the Marmara GPS network supported by World Bank Loan No: 3511-TU.

References

Ayhan, M.A., C. Demir, A. Kiliçoglu, I. Sanli, and S.M. Nakiboglu, Crustal motion around the western segment of the north Anatolian fault zone: geodetic measurements and geophysical interpretation, *International Union of Geodesy and Geophysics (IUGG99)*, 18-30 July, Birmingham, United Kingdom, 1999.

Barka, A., Slip distribution along the North Anatolian fault associated with the large earthquakes of the period 1939 to 1967, *Bull. Seismol. Soc. Am., 86*, 1238-1254, 1996.

Bürgmann, R., P. Segall, M. Lisowski, and J. Svarc, Postseismic strain following the 1989 Loma Prieta earthquake from GPS and leveling measurements, *J. Geophys. Res., 102*, 4933-4955, 1997.

Harris, R., and P. Segall, Detection of a locked zone at depth on the Parkfield, California segment of the San Andreas fault, *J. Geophys. Res., 92*, 7945-7962, 1987.

McClusky, S., S. Balassanian, A. Barka, C. Demir, S. Ergintav, I. Georgiev, O. Gurkan, M. Hamburger, K. Hurst, H. Kahle, K. Kastens, G. Kekelidze, R. King, V. Kotsev, O. Lenk, S. Mahmoud, A. Mishin, M. Nadariya, A. Ouzounis, D. Paradissis, Y. Peter, M. Prilepin, R. Reilinger, I. Sanli, H. Seger, A. Tealeb, M.N. Toksöz, and G. Veis, Global Positioning System constraints on plate kinematics and dynamics in the eastern Mediterranean and Caucusus, *J. Geophys. Res., 105*, 5695-5720, 2000.

Okada, Y., Surface deformation due to shear and tensile faults in a half-space, *Bull. Seismol. Soc. Am., 75*, 1135-1154, 1985.

Reilinger, R.E., S. Ergintav, R. Bürgmann, S. McClusky, O. Lenk, A. Barka, O. Gurkan, L. Hearn, K.L. Feigl, R. Cakmak, B. Aktug, H. Ozener, and M.N. Töksoz, Coseismic and postseismic fault slip for the 17 August 1999, M=7.5, Izmit, Turkey Earthquake, *Science*, *289*, 1519-1524, 2000.

Sengör, A.M.C., N. Görür, and F. Saroglu, Strike-slip faulting and related basin formation in zones of tectonic escape: Turkey as a case study, in *Strike-slip Faulting and Basin Formation*, edited by K.T. Biddle, and N. Christie-Blick, pp. 227-264, Society of Econ. Paleont. Min. Spec. Publ., 1985.

Stein, R.S., A.A. Barka, and J.H. Dietrich, Progressive failure on the North Anatolian fault since 1939 by earthquake stress triggering, *Geophys.J.Int. 128*, 594-604, 1997.

Straub, C., H.-G. Kahle, and C. Schindler, GPS and geologic estimates of the tectonic activity in the Marmara Sea region, NW Anatolia, *J. Geophys. Res., 102*, 27587-27601, 1997.

Toksöz, M.N., A.F. Shakal, and A.J. Michael, Space-time migration of earthquakes along the North Anatolian fault zone and seismic gaps, *Pure App. Geophys. 117*, 1258-1270, 1979.

Wells, D.L., and K.J. Coppersmith, New empirical relationships among magnitude, rupture length, rupture width, rupture area, and surface displacement, *Bull. Seismol. Soc. Am., 84*, 974-1002, 1994.

Yagi, Y., and M. Kikuchi, http://wwweic.eri.u-tokyo.ac.jp/yuji/trk2/Turkeyafter.html, 1999.

M. E. Ayhan, O. Lenk, B. Aktug, Department of Geodesy, General Command of Mapping, Ankara, Turkey

R. Bürgmann, Department of Earth and Planetary Science, 301 McCone Hall, University of California, Berkeley, Berkeley, CA 94720

S. McClusky, R. E. Reilinger, Department of Earth, Atmospheric, and Planetary Sciences, Massachusetts Institute of Technology, Cambridge, MA 02139

H. Herece, Department of Geology, General Directorate of Mineral Research and Exploration, Ankara, Turkey

(Received June 8, 2000; revised July 31, 2000;
accepted August 23, 2000.)